RADIATION EFFECTS OF INHOMOGENEOUS STRATOCUMULUS CLOUDS: 1. HORIZONTAL TRANSFER

G.A. Titov

Institute of Atmospheric Optics,
Siberian Branch of the Russian Academy of Sciences, Tomsk
Received May 13, 1996

Mathematical simulation is used to study the horizontal fluxes of solar radiation in stratocumulus clouds. Fractal cloud model with 1–D lognormal distribution and power-law spectrum is used, which correctly accounts for the distribution of liquid water in such clouds. It is shown that the radiative horizontal transfer, being zero in the plane-parallel model, is comparable (in the order of magnitude) with the other terms in the radiative energy balance equation. The horizontal transfer is responsible for non-unique dependence between the optical depth and the radiative properties of sampling volume (pixel). Slope β *of the energy spectrum (or fractal dimension) of optical depth is one of the fundamental parameters governing the horizontal radiative transfer: as* β *increases, the horizontal transfer decreases. The 1–D distribution of horizontal transfer is well fitted by the Gaussian distribution with zero mean.*

1. INTRODUCTION

Optical parameters of real clouds may have large horizontal gradients, so that a parallel solar flux incident on the top of the atmosphere is nonuniformly distributed in horizontal direction. This means that, within real clouds, simultaneously with upwelling and downwelling fluxes there may exist nonzero net horizontal flux coming out through sides of a sampling volume. Presently we know very little about this flux, poorly understanding its role in determining radiative transfer and its effect upon the accuracy of interpreting field data.

Calculations of horizontal fluxes in clouds of *finite* extents, located *regularly* (nonrandomly) in space, are presented in Refs. 1 and 2. A model of fair weather cumulus clouds, generated by Poisson point fluxes in space,[3] was used to study two-dimensional fields of albedo R, transmittance T, and their sum $R + T$. This model approximately accounts for the *statistical* nature of the effects caused by the cloud finite extents and approximates the clouds by inverted truncated paraboloids of rotation with exponential size distribution function. The net horizontal radiative flux, scaled to the incoming flux of visible solar radiation, is equal to $1 - R - T$. In absolute values this flux may be ~1 or greater, so it can play significant role in the interaction of radiation with clouds.

In the models used in Refs. 1–3 it is assumed that optical parameters are constant within the clouds, so that any nonzero net horizontal flux is caused only by geometrical effects: the presence of gaps, shadowing, escape of radiation through cloud sides, and multiple scattering between individual clouds. These effects are major physical factor determining the radiative properties of broken clouds whose horizontal extents are comparable to their depth. For such cloud systems, the variability of optical properties inside individual clouds can be neglected to the first approximation.

Also naturally occurring are clouds much larger horizontally than vertically. In this case, the geometrical effects listed above will only be essential for radiative transfer in a small (as compared to horizontal extent) region located near cloud side. For such clouds, the horizontal variability of radiative field is governed, on the average, by fluctuations of optical properties caused by liquid water content fluctuations, as well as by variations of cloud top and base heights.

In the present work, we study the influence of liquid water content fluctuations in stratocumulus clouds, completely covering the sky, on radiative horizontal flux.

2. ENERGY BALANCE EQUATION IN INHOMOGENEOUS CLOUDS

For integrity and clarity of presentation, we shall derive energy balance equations in inhomogeneous clouds, in which the radiative transfer is described by the three-dimensional equation

$$\omega\nabla I(\mathbf{r}, \omega) + \sigma(\mathbf{r})I(\mathbf{r}, \omega) = $$
$$= \omega_0(\mathbf{r})\sigma(\mathbf{r})\int_{4\pi} g(\mathbf{r}, \omega, \omega')I(\mathbf{r}, \omega')d\omega', \quad (1)$$

where $I(\mathbf{r}, \boldsymbol{\omega})$ is the intensity at the point $\mathbf{r}$ in direction $\boldsymbol{\omega}$, $\sigma(\mathbf{r})$ is the extinction coefficient, $\omega_0(\mathbf{r})$ is the single scattering albedo, and $g(\mathbf{r}, \boldsymbol{\omega}, \boldsymbol{\omega}')$ is the scattering phase function. Cloud and radiation characteristics are all wavelength dependent, which for convenience is not indicated here. With regard for the normalization condition on the scattering phase function, integration of Eq. (1) over full solid angle 4π leads to the energy conservation law of the form

$$\mathrm{div}\mathbf{F}(\mathbf{r}) = -F_\mathrm{a}(\mathbf{r}), \tag{2}$$

where the vector of power flux density $\mathbf{F}(\mathbf{r}) = (F_x, F_y, F_z) = \int\limits_{4\pi} \boldsymbol{\omega} I(\mathbf{r}, \boldsymbol{\omega})\, \mathrm{d}\boldsymbol{\omega}$ (W·m^{-2}) is equal to the sum of the net flux densities over three orthogonal coordinates; $F_\mathrm{a}(\mathbf{r}) = \sigma_\mathrm{a}(\mathbf{r}) \int\limits_{4\pi} I(\mathbf{r}, \boldsymbol{\omega})\, \mathrm{d}\boldsymbol{\omega}$ is the total absorbed power per unit volume; $\sigma_\mathrm{a}(\mathbf{r})$ is the absorption coefficient. Let us discuss the energy balance equation (2) in more detail.

For simplicity, we will not consider the reflection from the underlying surface and scattering and absorption of solar radiation by aerosol and atmospheric gases. Let clouds occupy the layer $h \le z \le H$ in the Cartesian coordinate system $OXYZ$. The parallel solar flux F_0 (W m^{-2}) is incident on the cloud top (plane $z = H$). We consider a spatial domain (pixel) bounded by the cloud upper and lower boundaries and the planes $x = \mathrm{const}$, $x + \Delta x = \mathrm{const}$, and $y = \mathrm{const}$, $y + \Delta y = \mathrm{const}$ (Fig. 1). Let us integrate equation (2) over the pixel volume

$$\int\limits_x^{x+\Delta x} \int\limits_y^{y+\Delta y} \int\limits_h^H \left\{ \frac{\partial F_x}{\partial x} + \frac{\partial F_y}{\partial y} + \frac{\partial F_z}{\partial z} \right\} \mathrm{d}x\, \mathrm{d}y\, \mathrm{d}z =$$

$$= -\int\limits_x^{x+\Delta x} \int\limits_y^{y+\Delta y} \int\limits_h^H F_\mathrm{a}(x, y, z)\, \mathrm{d}x\, \mathrm{d}y\, \mathrm{d}z. \tag{3}$$

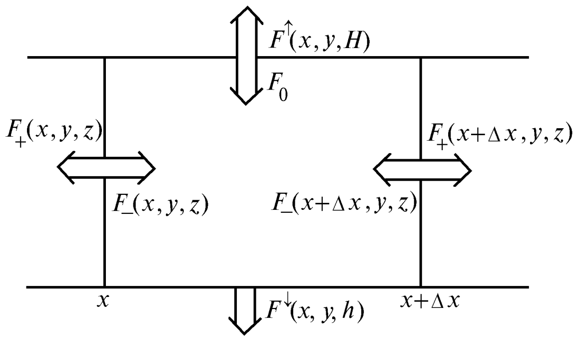

FIG. 1. Radiative fluxes coming out through the pixel top, base, and sides in the plane y = const.

Using Gauss divergence theorem, we convert the volume integral in the left side of the above equation to the surface integral

$$\int\limits_x^{x+\Delta x} \int\limits_y^{y+\Delta y} \int\limits_h^H \left\{ \frac{\partial F_x}{\partial x} + \frac{\partial F_y}{\partial y} + \frac{\partial F_z}{\partial z} \right\} \mathrm{d}x\, \mathrm{d}y\, \mathrm{d}z =$$

$$= \int\limits_S\int \{F_x \cos(\mathbf{n}, x) + F_y \cos(\mathbf{n}, y) + F_z \cos(\mathbf{n}, z)\}\, \mathrm{d}S, \tag{4}$$

where S is the closed surface bounding the pixel and $\mathbf{n}$ is the normal outward pointing vector. We introduce the following notations (Fig. 1):

– $F^{\uparrow}(x, y, H)$ is the flux density of radiation reflected at the point (x, y, H);

– $F^{\downarrow}(x, y, h)$ is the flux density of radiation transmitted at the point (x, y, h);

– $F_\mathrm{e}(x_*, y, z) = F_+(x_*, y, z) - F_-(x_*, y, z)$, $x_* = x, x + \Delta x$, is the net flux density of radiation passing through the pixel side (either plane $x = \mathrm{const}$ or $x + \Delta x = \mathrm{const}$) at the point (x_*, y, z);

– $F_\mathrm{e}(x, y_*, z) = F_+(x, y_*, z) - F_-(x, y_*, z)$,

$y_* = y$, $y + \Delta y$, is the net flux density of radiation passing through the pixel side (either plane $y = \mathrm{const}$ or $y + \Delta y = \mathrm{const}$) at the point (x, y_*, z).

With regard for the notations and the above assumptions, the surface integral in Eq. (4) takes the form:

$$\int\limits_S\int \{F_x \cos(\mathbf{n}, x) + F_y \cos(\mathbf{n}, y) + F_z \cos(\mathbf{n}, z)\}\, \mathrm{d}S =$$

$$= \int\limits_y^{y+\Delta y} \int\limits_h^H \{F_\mathrm{e}(x, y, z) + F_\mathrm{e}(x + \Delta x, y, z)\}\, \mathrm{d}y\, \mathrm{d}z +$$

$$+ \int\limits_x^{x+\Delta x} \int\limits_h^H \{F_\mathrm{e}(x, y, z) + F_\mathrm{e}(x, y + \Delta y, z)\}\, \mathrm{d}x\, \mathrm{d}z +$$

$$+ \int\limits_x^{x+\Delta x} \int\limits_y^{y+\Delta y} \{F^{\uparrow}(x, y, H) - F_0\}\, \mathrm{d}x\, \mathrm{d}y +$$

$$+ \int\limits_x^{x+\Delta x} \int\limits_y^{y+\Delta y} F^{\downarrow}(x, y, h)\, \mathrm{d}x\, \mathrm{d}y. \tag{5}$$

As follows from Eqs. (3)–(5), the law of energy conservation in three-dimensional clouds can be written out as

$$R(x, y) + T(x, y) + A(x, y) = 1 - E(x, y). \tag{6}$$

Here $F_0 \Delta x \Delta y$ has the meaning of the flux of solar radiation reaching the pixel;

$$R(x, y)= \int_x^{x+\Delta x} \int_y^{y+\Delta y} F^{\uparrow}(x, y, H)\mathrm{d}x\mathrm{d}y / F_0\, \Delta x\, \Delta y$$ is albedo;

$$T(x, y) = \int_x^{x+\Delta x} \int_y^{y+\Delta y} F^{\downarrow}(x, y, H)\, \mathrm{d}x\, \mathrm{d}y / F_0\, \Delta x\, \Delta y$$

is transmittance;

$$A(x, y) = \int_x^{x+\Delta x} \int_y^{y+\Delta y} \int_h^H F_{\mathrm{a}}(x, y, z)\, \mathrm{d}x\, \mathrm{d}y\, \mathrm{d}z / F_0\, \Delta x\, \Delta y$$

is absorptance; and

$$e\,(x, y) = \int_y^{y+\Delta y} \int_h^H \{F_{\mathrm{e}}(x, y, z) +$$
$$+ F_{\mathrm{e}}(x + \Delta x, y, z)\, \mathrm{d}y\, \mathrm{d}z / F_0\, \Delta x\, \Delta y +$$
$$+ \int_x^{x+\Delta x} \int_h^H \{F_{\mathrm{e}}(x, y, z) +$$
$$+ F_{\mathrm{e}}(x, y + \Delta y, z)\}\, \mathrm{d}x\, \mathrm{d}z / F_0\, \Delta x\, \Delta y$$

is the ratio of the net radiative flux, lost ($e\,(x, y) > 0$) or gained ($e\,(x, y) < 0$) through the pixel sides, to the incoming flux. For convenience, $e\,(x, y)$ will be termed the horizontal transfer. According to Eq. (6), the amount of radiative energy reflected, transmitted, and absorbed by a pixel may be either greater or less than unity, depending on the sign of $e\,(x, y)$. Dependence of this sign on the optical parameters of a given pixel and neighboring ones, as well as on the solar zenith angle, is discussed in Section 4.

Radiative flux densities are limited functions, hence it follows from the definitions of albedo, transmittance, absorptance, and horizontal transfer that $\lim\limits_{\substack{\Delta x \to \infty \\ \Delta y \to \infty}} R(x,y)=\langle R\rangle$, $\lim\limits_{\substack{\Delta x \to \infty \\ \Delta y \to \infty}} T(x,y)=\langle T\rangle$, $\lim\limits_{\substack{\Delta x \to \infty \\ \Delta y \to \infty}} A(x,y)=\langle A\rangle$ and $\lim\limits_{\substack{\Delta x \to \infty \\ \Delta y \to \infty}} E(x, y) = 0$. Here and below, $\langle\cdot\rangle$ denotes an average over space.

We let L denote the mean length of photon lateral migration in clouds. Major contributors to $e\,(x, y)$ are the sections of a pixel located near pixel sides and having lengths on the order of L. As pixel extents grow, $F_0\Delta x\Delta y$ increases linearly in each of Δx and Δy, whereas integrals used to define the horizontal transfer increase for $\Delta x, \Delta y \le L$ and are almost unchanged when $\Delta x, \Delta y > L$. For this reason, at $\Delta x, \Delta y \gg L$ the horizontal transfer $e\,(x, y) \ll 1$, and equation (6) can be written as

$$R(x, y) + T(x, y) + A(x, y) = 1. \tag{7}$$

Given $\Delta x, \Delta y \sim L$, averaging Eq. (6) over such number $N_x N_y$ of pixels that $N_x\, \Delta x \gg L$, $N_y\, \Delta y \gg L$ gives $\langle e\rangle = \frac{1}{N_x N_y} \sum\limits_{k=1}^{N_x} \sum\limits_{m=1}^{N_y} E(x_k, y_m) \approx 0$, so that equation of the type of Eq. (7) is again valid

$$\langle R\rangle + \langle T\rangle + \langle A\rangle = 1. \tag{8}$$

As seen, space averaging is equivalent to pixel stretching. This result stems from albedo, transmittance, absorptance, and radiative horizontal transfer definitions. In the presence of reflecting surface, the transmittance in Eqs. (6)–(8) must be replaced by the net transmitted flux scaled to the incoming solar radiation flux.

The radiative transfer in inhomogeneous clouds is calculated using independent pixel approximation (IPA),[4,5] whose accuracy is estimated in Ref. 6. The essence of this approximation is that the radiative properties of each pixel depend only on its own vertical optical thickness, and not on the optical thickness of neighboring pixels. In other words, in IPA we neglect the horizontal radiative transfer, i.e., for *any* pixel we assume $e\,(x, y) \equiv 0$ and *always* use energy balance equation (7). In Ref. 7 we show that the neglect of horizontal transfer leads to uncontrollable errors when determining cloud absorption from field data.

3. CLOUD MODEL AND METHOD OF SOLUTION

Two-parameterical fractal models generated by multiplicative cascade processes provide realistic simulation of the observed distribution of liquid water in marine stratocumulus clouds Sc.[4–6,8] Analysis of FIRE data for Sc over California has shown that the field of optical depth has one-point lognormal distribution and power-law energy spectrum $f(k) \sim k^{-\beta}$ with exponent $\beta = 5/3$ corresponding to the Kolmogorov–Obukhov law.

Instead of cascade processes, for constructing numerical realizations of the distribution of optical depth we used spectral methods of simulating random processes (fields) with one-dimensional lognormal distribution and power-law.[9] The spectral model of optical depth field has the following advantages over the cascade one.

– Input parameters in spectral model have more customary statistical meaning: mean $\langle\tau\rangle$, variance D_τ, and the exponent of the power-law energy spectrum β.

– In cascade model the *peacewise constant* cloud field is constructed in a fixed, horizontally *finite* volume, whereas algorithms based on spectral methods determine *continuous* cloud fields in a horizontally *infinite* volume.

– Spectral methods allow simulation of random fields with an arbitrary exponent β of the power-law energy spectrum, whereas with the use of cascade processes one can construct realizations of the random fields with $\beta \le 2$.

For less expensive computation of cloud radiative properties, we use one-dimensional model of optical depth that depends on the horizontal coordinate x alone. In other words, the optical depth is modeled as a random process with one-dimensional lognormal distribution and power-law spectrum. A continuous realization of this process is divided into $N_x = 2^{nx}$ pixels of the same horizontal extent $\Delta. = 0.05$ km. For each pixel an optical depth τ_i, $i = 1, \ldots, N_x$, is assigned as a value of the random process at the point corresponding to the left-hand side of the pixel, and then the pixel extinction coefficient is calculated as $\sigma_i = \tau_i/\Delta H$, where $\Delta H = H - h$ is the cloud layer thickness. In calculations we used $\langle\tau\rangle = 13$, $D_\tau = 29$, $\beta = 5/3$, $h = 1.0$ km and $\Delta H = 0.3$ km, which are typical for marine Sc.[5] unless otherwise specified.

Numerical simulation of the interaction of solar radiation with inhomogeneous stratocumulus clouds is performed with the following assumptions and parameter values. The underlying surface has albedo A_s and reflects according to Lambert's law. The calculation results presented are for $A_s = 0$ and 0.4 that correspond roughly to albedo of ocean and desert, respectively. Scattering phase function for C1 cloud[10] is calculated from the Mie theory for a wavelength of 0.69 μm and a single scattering albedo of $\omega_0 = 1.0$. Atmospheric aerosol is optically thin as compared to $\langle\tau\rangle$ of clouds, so its influence was neglected. The number of pixels is $N_x = 2^{12} = 4096$ and the length of the cloud realization is 204.8 km. The equation of radiative transfer in inhomogeneous clouds was solved by the Monte Carlo method using periodic boundary conditions. The solar incidence is defined by zenith $\xi_\odot$ and azimuthal $\varphi_\odot$ angles. The latter is measured from OX-axis and set to zero throughout the computation. For each pixel we calculated albedo and transmittance T_b at the cloud top (plane $z = H$) and base (plane $z = h$) heights, respectively; and additionally we calculated transmittance T_0 at the underlying surface level. The mean relative error in albedo, transmittance, and absorptance computations did not exceed 0.6–0.7%, while the maximum error was within 1.0 to 1.5%.

4. HORIZONTAL RADIATIVE TRANSFER

In the plane-parallel model, the radiative properties of clouds are *uniquely* determined by their optical parameters. Obviously, this unique dependence will also hold in IPA[4,5], since it calculates the radiative properties of each pixel using radiative transfer equation within plane-parallel model while ignoring interaction of radiative fields of individual pixels. In IPA, the albedo R_{IPA} and transmittance T_{IPA} can be calculated for each pixel using the formula which for conservative scattering has the form[5]

$$R_{\mathrm{IPA}}(\tau;\, \xi_\odot,\, g) = 1 - T_{\mathrm{IPA}}(\tau;\, \xi_\odot,\, g);$$

$$T_{\mathrm{IPA}}(\tau;\, \xi_\odot,\, g) = \\ = \frac{\delta(\xi_\odot) + [1 - \delta(\xi_\odot)]\exp[-\tau/|a(\xi_\odot)|]}{1 + \gamma(g)\tau}, \qquad (9)$$

where τ is the pixel optical depth, $\xi_\odot$ is the solar zenith angle, and g is the asymmetry parameter of the scattering phase function. Below we use the following values of the functions: $\delta(60°) = 0.8$, $a(60°) = 0.8$ and $\gamma(g) = 0.13$.

Quite the contrary situation occurs for real inhomogeneous clouds when the pixel size is less than or nearly equal to the mean length of photon horizontal migration. Owing to the inhomogeneity of radiative horizontal fluxes, two pixels having the same optical thickness but different optical parameters of neighboring pixels may possess different albedos and transmittances (Figs. 2*a*,*b*). For instance, for pixels with an optical depth of 10, T_0 may differ by almost a factor of two.

In absolute values, the horizontal transfer may reach 20% of solar irradiance (Fig. 2*c*), i.e., be of about the same order as the other terms in the energy balance equation (6). Noteworthy, so high E values are obtained for overcast stratocumulus clouds, whose optical properties vary *only due* to fluctuations in liquid water content. Inclusion of the stochastic geometry of cloud upper and lower boundaries will increase the horizontal gradients of optical parameters and, hence, will result in higher peak values of $|E|$. This seems to be very important result for it clearly illustrates the fact that the horizontal radiative transfer may play significant role in *any* cloud systems: an isolated cloud of finite extents, field of broken clouds including cumulus, and stratiform clouds with horizontally variable optical properties.

Pixels with $\tau_i < 5$ have horizontal optical thickness $\tau_{i,x} = \tau_i \cdot \Delta x/\Delta H < 1$, i.e., they are optically thin in the horizontal direction. Most photons traverse such pixels without scatter, so they predominantly loose $(e(x_i) > 0)$ radiation through their sides (Fig. 2c). The reverse is true for optically thick pixels, with $\tau_i > 25$ and $\tau_{i,x} > 5$. From Fig. 2 we see that the horizontal transfer gives rise to nonunique dependence of R and T_0 on the pixel optical depth: the maximum "scatter" in R and T_0 occurs in pixels having largest $|e|$ values. The larger the pixel optical depth, the smaller the region located near pixel sides and playing major part in the radiation interaction of pixels; thus the less both $|e|$ and, hence, the "spread" in R and T_0 values.

To better understand the dependence of horizontal transfer on the optical thickness of a given pixel and neighboring ones, in E realization we found the pixels with E reaching its maximum ($e_{\max} > 0$) and minimum ($e_{\min} < 0$) values. Fragments of E and τ realizations including such pixels are shown in Fig. 3. Pixels loosing radiative energy most are optically thin and located in shadows ($\xi_{\odot} = 60°$) of neighboring, optically dense pixels (Fig. 3*a*). This can be explained by the fact that, due to large optical depth of the "shadowing" pixels, only a small fraction of radiation incident on their tops reaches the pixels with $e_{\max}$. The reverse is true for pixels with $e_{\max}$: because of the small optical thickness and strong forward peak of the scattering phase function, major portion of solar radiation impinging on the tops of such pixels leaks through their sides, predominately into the neighboring pixels located "on the way" of the incident solar radiation.

Horizontal transfer reaches its minimum values on sunlit sides of the pixels possessing relatively large optical thicknesses and having an optically thin region in front of them (Fig. 3*b*). The incoming solar radiation passes through this region, adding substantially to the amount of radiative energy available for scattering and absorption by the optically thick pixels.

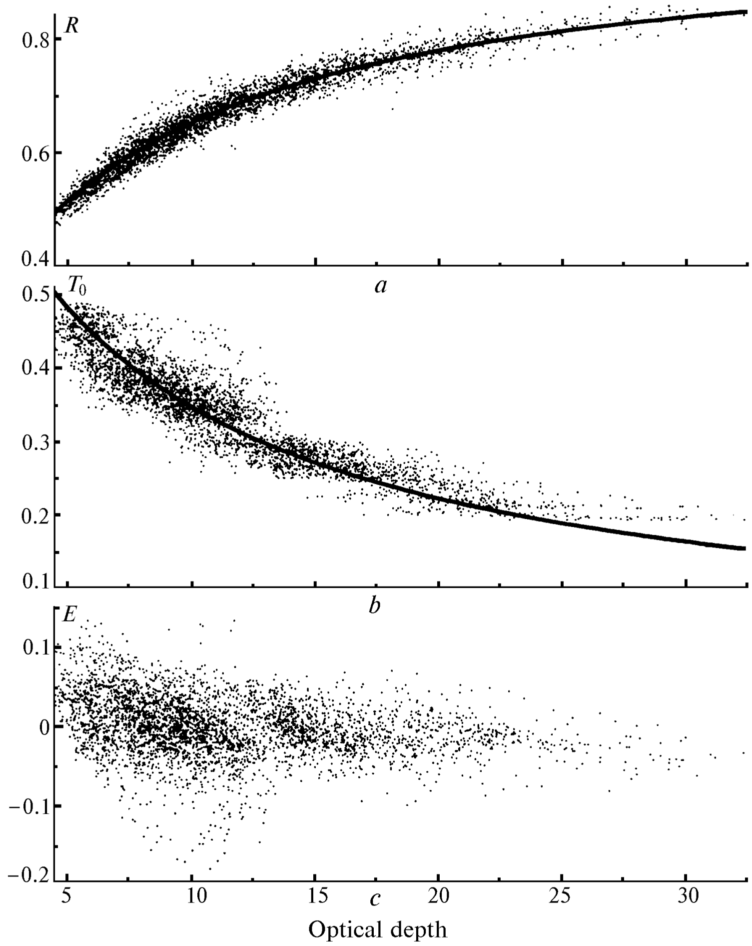

FIG. 2. Albedo R (a), transmittance T_0 at the underlying surface level (b), and the horizontal transfer e (c) as functions of pixel optical depth for solar zenith angle $\xi_{\odot} = 60°$ and surface albedo $A_s = 0$ (ocean). Solid lines are for albedo and transmittance calculated in IPA by formula (9).

Figure 3 clearly illustrates how the horizontal transfer is affected by the optical parameters of the neighboring pixels. Optically dense pixels presented in Figs. 3*a* and 3*b* have approximately the same optical depth. In the first instance (Fig. 3*a*), they predominantly loose radiation ($e > 0$), due to the optically thick region in front of them. In the second instance (Fig. 3*b*), they gain ($e < 0$) extra radiation from the optically thin region in front of them. Note that the scale on which E changes its sign ranges from hundreds of meters to 1–2 km.

Figure 4 shows one-point probability densities of horizontal transfer obtained using statistical analysis of numerical realizations $e(._i)$, $i = 1, \ldots, 4096$. We recall that, when averaged over complete realization, $\langle e \rangle = 0$ for any problem parameters. Strong anisotropy of the cloud scattering phase function is responsible for the fact that, as the solar zenith angle increases, the distribution of E broadens, i.e., the variance of E increases. The probability density $p(e)$ is well fitted by the Gaussian function. The results of

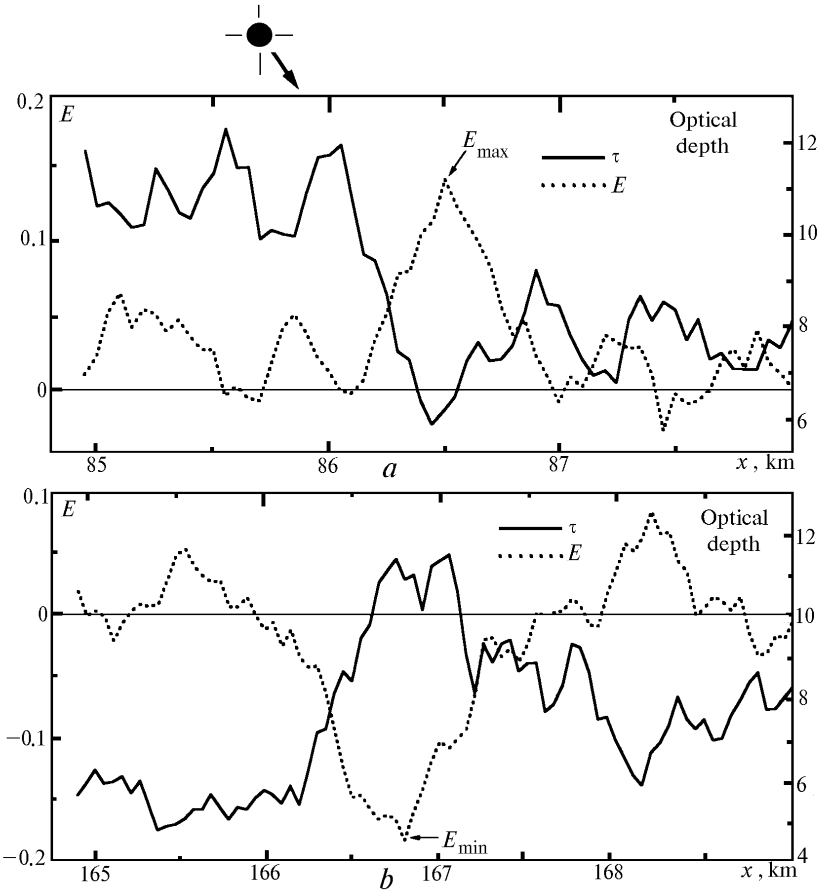

FIG. y. Segments of the cloud realization on which horizontal transfer reaches its maximum (a) and minimum (b) values, with solar zenith angle $\xi_\odot = 60°$ and surface albedo $A_s = 0$ (ocean).

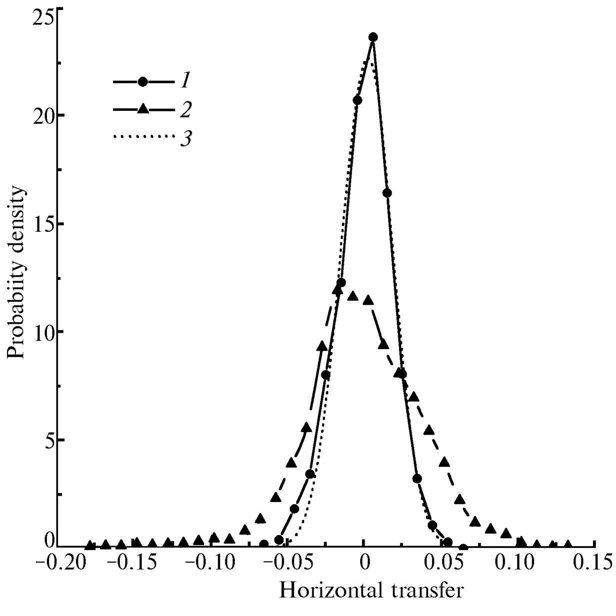

FIG. 4. Probability densities of the horizontal transfer for $A_s = 0$ (ocean) and solar zenith angles of 0 (1) and 60° (2); a fit by the Gaussian probability density function ($\xi_\odot = 0°$) (y).

numerical simulation show that $p(e)$ depends weakly on the underlying surface albedo.

Figure 5 presents numerical realizations of the random functions $\tau(.)$, $R(x)$, $T_0(x)$ and $e(x)$, obtained with fixed parameters of the one-point lognormal distribution and different values of the exponent β, characterizing the slope of the power-law energy spectrum of optical depth. It is well known[11] that fractal dimension D of the plot of $\tau(.)$, considered as a random geometrical object in the two-dimensional space, changes from one (differentiable process) to two (everywhere discontinuous process). The fractal dimension is a measure of smoothness: the greater D, the less smooth is the function $\tau(.)$. At $\beta = 5/3$, $D = (5 - \beta)/2 = 5/3$ (Ref. 8), and the plot of $\tau(.)$ appears as some envelope, defining the variability of $\tau(.)$ at macroscales (~10 km and larger), upon which small-scale fluctuations (from hundreds of meters to several kilometers) are superimposed. We see that $\tau(.)$ may have large "jumps" for small increments in the argument (Fig. 5*a*). When $\beta = 2.9$, $\tau(.)$ appears as much smoother function; while at $\beta = 3.0$, $D = 1$, so that $\tau(.)$ would be a differentiable function.

As β increases from 5/3 to 2.9, the functions $R(.)$ and $T_0(.)$, being nonlinear transformations of $\tau(.)$, also become smoother (Figs. 5*b*,*c*). The form of this transformation is determined by the radiative transfer equation. Albedo and transmittance are sensitive to both macro- and microscale fluctuations of $\tau(.)$. It should be noted that, at $\beta = 5/3$, $R(.)$ appears much less smooth function than $T_0(.)$. This effect can be explained as follows. First, multiple scattering smoothes out the radiative field, thus causing scaling breaks in the energy spectra of albedo[12] and transmittance.[13] Second, the radiative field smoothness depends on the distance between detector measuring radiation and a corresponding cloud boundary (geometrical factor). As the distance increases, so too does the spatial volume falling within the detector field of view, therefore the radiative field is additionally smoothed. The geometrical factor can explain the above effect: $R(.)$ is "measured" at the cloud top altitude, while $T_0(.)$ is “measuredB at the underlying surface level.

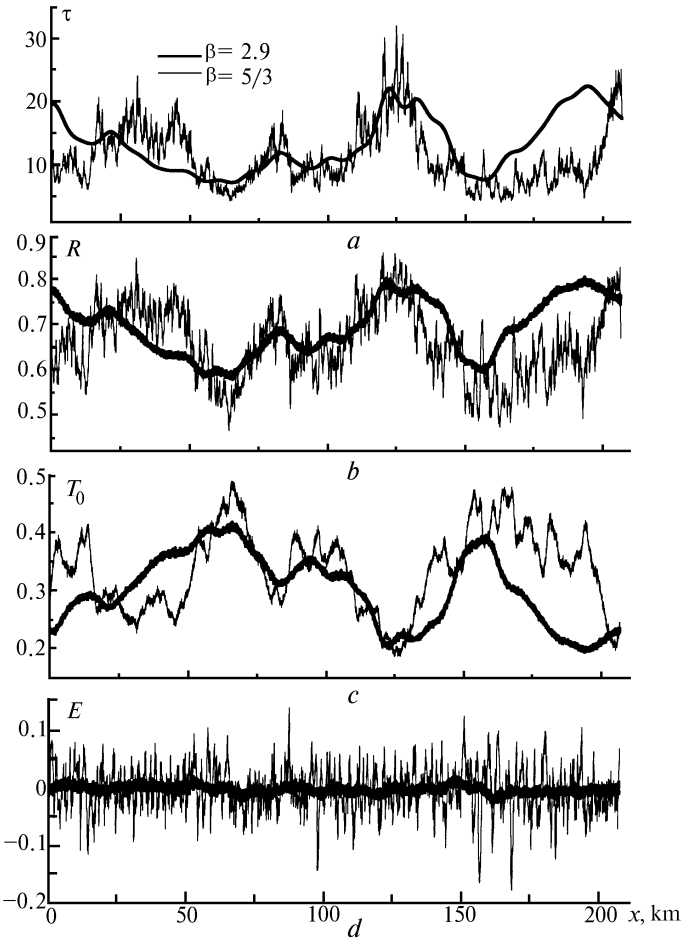

FIG. 5. Numerical realizations of optical depth (a), albedo (b), transmittance T_0 (c), and horizontal transfer (d), for $\xi_\odot = 60°$, $A_s = 0$ (ocean), and different slopes β of the power-law energy spectrum of τ.

Because of the large cloud optical depth, radiation leaking out through the pixel sides interacts with nearby pixels only, and cannot interact with pixels ~10 km or more apart. This explains the insensitivity of $e(.)$ to the macroscale fluctuations of optical depth (Fig. 5*d*). Further, at $\beta = 2.9$, $\tau(.)$ is a smooth function, and the neighboring pixels differ little in optical depth. For each pixel, the loss and gain of radiative energy through pixel sides nearly compensate each other, $e(.) \approx 0$, so that simpler energy balance equation (7) can be used. Thus, the slope of the energy spectrum (or the fractal dimension) of cloud optical depth represents one of the fundamental parameters governing the radiative horizontal transfer in inhomogeneous clouds.

5. CONCLUSION

The energy balance equation in inhomogeneous clouds contains a term (the radiative horizontal transfer) that describes the net radiative flux lost or gained through the sides of a sampling volume (pixel). Because of the horizontal transfer, the uniform incident solar flux is nonuniformly distributed over space.

In typical stratocumulus clouds, the radiative horizontal transfer, being zero in the plane-parallel model and IPA, is comparable (in the order of magnitude) with albedo, transmittance, and absorptance. The horizontal transfer is responsible for the fact that the radiative field depends on optical properties of both a given pixel and neighboring ones. In other words, because of the horizontal transfer, there is no one-to-one dependence between the optical depth and radiative properties of a given pixel. One of the key parameters governing the radiative horizontal transfer is the slope β of the energy spectrum (or the fractal dimension) of cloud optical depth: as β increases, the horizontal transfer diminishes. One-point distribution of horizontal transfer is well fitted by the Gaussian distribution with zero mean.

ACKNOWLEDGMENTS

The support from the DOE's ARM Program (contract No. 350114-A-Q1) and the Russian Foundation for Fundamental Research (grant No. 96-05-64275) is appreciated.

REFERENCES

1. R.M. Welch, S.K. Cox, and J.M. Davis,: "*Solar radiation and clouds*B, Meteor. Monogr., No. 39, Amer. Meteor. Soc. (1980), 93 pp.
2. T. Hayasaka, N. Kikuchi, and M. Tanaka, J. Appl. Meteorol. **34**, 1047–1055 (1995).
3. G.A.Titov, Atmos. Oceanic Opt. **9**, No. 1, 1–7 (1996).
4. R.F. Cahalan, in: *Advances in Remote Sensing Retrieval Methods* (Deepak Pub., 1989), pp. 371–388.
5. R.F. Cahalan, W. Ridgway, W.J. Wiscombe, T.L. Bell, and J.B. Snider, J. Atmos. Sci. **51**, No. 16, 2434–2455 (1994).
6. R.F. Cahalan, W. Ridgway, W.J. Wiscombe, S. Gollmer, and S. Harshvardhan, J. Atmos. Sci. **51**, 3776–3790 (1994).
7. G.A. Titov, Atmos. Oceanic Opt. **9**, No. 10, 833–838 (1996).
8. A. Marshak, A. Davis, R.F. Cahalan, and W.J. Wiscombe, Phys. Rev. **E49**, 55–79 (1994).
9. S.M. Prigarin, and G.A. Titov, *Atmos. Oceanic Opt.* **9**, No. 7, 629–635 (1996).
10. D. Deirmendjian, *Electromagnetic Scattering on Spherical Polydispersions* (American Elsevier, New York, 1969).
11. B.B. Mandelbrot, *Fractals: Form, Change, and Dimension* (W.H. Freeman and Co., San Francisco, 1977), 365 pp.
12. A. Davis, A. Marshak, R.F. Cahalan, and W.J. Wiscombe, J. Atmos. Sci., 1996 (in press).
13. G.A. Titov, and E.I. Kasyanov, Atmos. Oceanic Opt. **8**, No. 12, 1028–1034 (1995).